

## Corrosion Resistance Evaluation of Acrylic Coating Incorporated With Henna Leaves Extract

Mohammad Fakhratul Ridwan Zulkifli<sup>a\*</sup>, Mohd Sabri Mohd Ghazali<sup>b</sup>, Mohd Ikmar Nizam Mohamad Isa<sup>c,d</sup>,  
Suriani Mat Jusoh<sup>a</sup>, Akihiro Yabuki<sup>e</sup> & Wan Mohd Norsani Wan Nik<sup>a</sup>

<sup>a</sup>Materials and Corrosion Research Group, Faculty of Ocean Engineering Technology and Informatics, Universiti Malaysia Terengganu, Malaysia

<sup>b</sup>Advanced Nano Materials (AnoMa) Research Group, Faculty of Science and Marine Environment, Universiti Malaysia Terengganu, Malaysia

<sup>c</sup>Frontier Materials Research, Faculty of Science and Technology, Universiti Sains Islam Malaysia, Malaysia

<sup>d</sup>Advanced Nano Materials (AnoMa) Research Group, Advanced Materials Team, Ionic State Analysis (ISA) Laboratory, Faculty of Science and Marine Environment, Universiti Malaysia Terengganu, Malaysia

<sup>e</sup>Graduate School of Engineering, Hiroshima University, Japan

\*Corresponding author: fakhratulz@umt.edu.my

Received 21 August 2019, Received in revised form 14 November 2019

Accepted 22 January 2020, Available online 30 May 2020

### ABSTRACT

The study employs optical measurements, electrochemical studies and mechanism evaluations of an acrylic coating incorporated with henna leaves extract (HLE) at ambient temperature. The effect of concentrations variation of HLE in acrylic coating was investigated and acrylic coating with 0.2 wt/vol% (AC2) of HLE had the best performance protecting aluminium alloy 5083 from corrosion. Characterization through Fourier Transform Infrared Spectroscopy (FTIR) demonstrates the association of the carbonyl group of lawsone with the acrylic resin polymer via chain scission. A further deconvolution method was used in the range of 1550 – 1720  $\text{cm}^{-1}$  and the complexation between HLE and acrylic coating was observed due to the shifting of carbonyl peak. AC2 shows the lowest water permeability value due to the compact structure and high density of the HLE colloidal system. Coating resistance shows an increasing trend upon incorporation of HLE and reaches the maximum resistance at AC2. A circuit fitting analysis of electrochemical impedance spectroscopy (EIS) indicates that all coated samples is represented by  $[(R_f Q_{dl})(R_{ct} Q_{dl})(W)]$  circuit. Warburg impedance,  $W$  for AC2 shows the lowest value ( $1.21 \times 10^{-7} \Omega \cdot \text{s}^{-1/2}$ ) in comparison to the other samples which indicates lower speed of diffusion. Suggested mechanism shows that HLE in AC2 was formed in a close pack structured in which providing a greater barrier effect towards corrosion susceptibility of aluminium alloy 5083.

**Keywords:** Acrylic resin coating; Corrosion additive; Electrochemical; Optical studies

### INTRODUCTION

Corrosion prevention of aluminium alloy has attracted enormous attention from researchers due to its wide application as a structural material (Othman et al. 2018). For marine grade aluminium, the exposure of the metal to seawater is a real concern where diffusion of water that contains corrosive ion and dissolved oxygen will initiate the pit growth on the aluminium surface. Organic coating such as acrylic resin is one of the prevention methods used to overcome corrosion because of their durability and low cost (Akbarinezhad et al. 2014; Papaj et al. 2014). It provides an insulation layer on the surface which acts as a barrier from corrosive ions, water and oxygen. This insulating layer however may also obstruct the path of electron and cause several problems in post-processes.

Incorporating various additive can be a tolerance approach to enhance the corrosion resistance of the polymeric coating. The physical and chemical

properties of additive molecule assist the adsorption process due to the electronic density of donor atoms and the possible steric effects (Khaled & Hackerman, 2003). Henna leaves extract (HLE) has been reported to exhibit various biological activities such as antimicrobial, anti-oxidant, fungitoxic and anti-corrosion. According to several literatures, *Lawsonia inermis* exhibits an exquisite inhibition effect towards corrosion (Ostovari et al. 2009; Rajendran et al. 2009; Motalebi et al., 2012). The presence of 2-hydroxy-1,4-naphthoquinone in *Lawsonia inermis* contributes to the important activities such as anti-oxidant, anti-inflammatory, anti-cancer and anti-corrosion (Abulyazid et al. 2013; Jeyaseelan et al. 2012; Salunke-Gawali et al. 2012; Buchweishaija, 2009).

Due to its excellence as a corrosion inhibitor and wide range of applications, HLE has been chosen in this study. Incorporation of HLE in acrylic resin coating was evaluated via optical and

electrochemical measurements. The effect of concentrations on the new coating system was evaluated and it was found that it is capable to protect aluminium alloy 5083 (AA5083) from corrosion attack.

#### METHODOLOGY

##### Surface preparation of aluminium alloy 5083 (AA5083)

AA5083 was used in square shape with the dimension of 25 mm x 25 mm x 3 mm and polished by using emery paper with different grades (600, 900 and 1200). The samples were cleaned with acetone and rinsed with distilled water, dried in the air and then stored in desiccators prior to use. The composition of AA5083 is tabulated in Table 1 (Ashjari et al. 2015).

TABLE 1. Composition of aluminium alloy 5083 (AA5083)

Element	Mg	Mn	Fe	Si	Zn	Cr	Ti	Cu	Al
Weight percent, wt%	4.5	0.7	0.4	0.4	0.25	0.15	0.15	0.1	Remaining

##### Preparation of coating

The fresh leaves of henna were dried at room temperature and then crushed to powder form. Henna powder was soaked in ethanol for a week. Then, the mixture was extracted by using a rotary evaporator. The residue left in the flush was used in accordance with coating system and later was referred as henna leave extract (HLE). The acrylic resin coating was purchased locally. The incorporation of HLE into the acrylic resin coating was made in according to weight per volume percent (wt/vol %) where mass of of the dissolved solute is divided by the volume of the entire solution in milliliters. The range of wt/vol% used in this study was 0.1 – 0.4 wt/vol %. The mixtures were stirred for 2 hours and were coated on aluminium alloy by using brushes having a thickness of  $25 \pm 5 \mu\text{m}$ . Corrosion test was performed by using seawater collected at aquatrop hatchery, Universiti Malaysia Terengganu. To easily identify the coating system, the following abbreviation as tabulated in Table 2 should be referred.

TABLE 2. Abbreviation of a coating system

Coating mixture	Abbreviation
Acrylic resin	AC
Acrylic resin + 0.1 wt/vol%	AC1
Acrylic resin + 0.2 wt/vol%	AC2
Acrylic resin + 0.3 wt/vol%	AC3
Acrylic resin + 0.4 wt/vol%	AC4

##### Fourier transform infrared (FTIR)

Fourier transform infrared (FTIR) was carried out using Thermo Nicolet 380 FTIR Spectrometer. The spectrometer was used to identify the functional group of HLE by observing at the vibrational motion of bonds in molecules. The subsequent effect after the incorporation was studied as well. This

spectrometer was equipped with an Attenuated Total Reflection (ATR) accessory with a germanium crystal. The sample was put on germanium crystal and infrared light was passed through the sample with the frequency ranging from 3960 to 660  $\text{cm}^{-1}$  with spectral resolution of 4  $\text{cm}^{-1}$  (Samsudin et al. 2012). The FTIR data were recorded in the transmittance mode. The transmittance and reflectance of the infrared rays at different frequencies were translated into an IR absorption plot consisting of reverse peaks. The spectral pattern was analysed and matched according to IR absorption table.

##### Water permeability study

Acrylic films with uniform thickness of 0.582 mm were cut into 0.0001  $\text{m}^2$  and soaked in seawater for the duration of 300 minutes. The reading of water uptake was taken every 60 minutes of interval by using JA-303H analytical balance (readability: 0.001g). Water transmission rate was calculated based on the following equation (Kucera et al. 2009):

$$WTR = \left(\frac{G}{t}\right)/A \quad (1)$$

where  $G$  is the weight changes of the film in gram,  $t$  is the time of film soak in seawater in minute, and  $A$  is the area of the film in  $\text{m}^2$ .

##### Electrochemical impedance spectroscopy (EIS)

EIS was used to study the impedance characteristic as well as capacitance behaviour of AA5083 in the presence and absence coating. The EIS measurement was conducted by using alternating current signal of impedance measurements by using Autolab PGSTAT302N with respect to the open circuit potential (OCP). All the potentials referred were relative to a saturated calomel electrode (SCE). The impedance measurements were conducted over a frequency range of 10000 Hz down to 0.01 Hz. The

results were analysed using NOVA 1.10 electrochemical program.

## RESULTS AND DISCUSSION

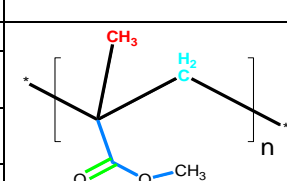
### Fourier Transform Infrared (FTIR) Technique

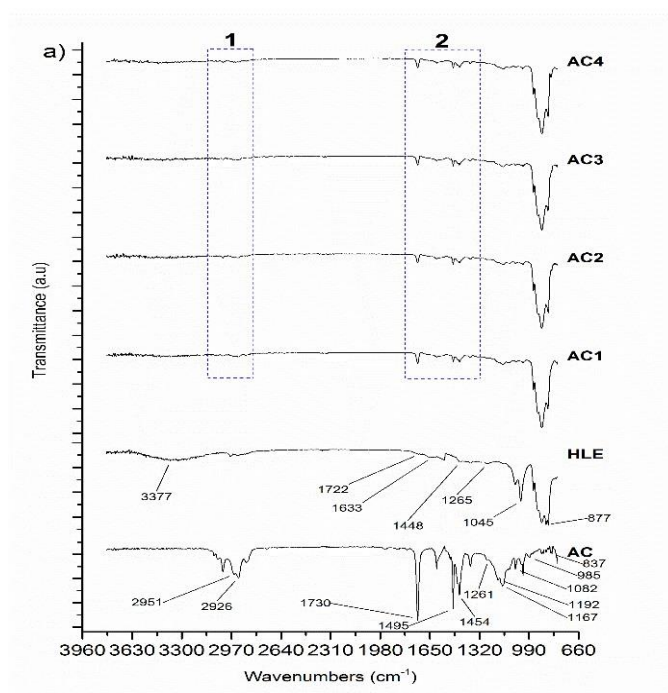
FTIR spectrum of acrylic coating (AC), HLE and AC incorporated with HLE in the range of 660 – 3960  $\text{cm}^{-1}$  are depicted in Figure 1a. HLE spectrum showed a broad band centered at 3376  $\text{cm}^{-1}$  and it was attributed to the stretching hydroxyl (OH) group (Gaaz et al. 2017). The stretching vibration of C=O was observed at 1722  $\text{cm}^{-1}$  and 1633  $\text{cm}^{-1}$ . The peak at 1448  $\text{cm}^{-1}$  was attributed to the aromatic stretching band C=C while a few bands at 1265  $\text{cm}^{-1}$ , 1045  $\text{cm}^{-1}$

and 877  $\text{cm}^{-1}$  were attributed to the C-O stretching and aromatic ring, respectively.

C-C-O-C stretching vibration of AC was represented by a distinct band around 1166, 1195 and 1261  $\text{cm}^{-1}$ . A carbonyl functional group C=O stretching is represented by a band at 1729  $\text{cm}^{-1}$  while a peak at 1494  $\text{cm}^{-1}$  was attributed to the methyl group vibration. Two peaks at 2925 and 2950  $\text{cm}^{-1}$  were attributed to the C-H stretching while CH<sub>2</sub> stretching can be observed at 1454  $\text{cm}^{-1}$ . In the fingerprint region, few peaks at 836, 985 and 1081  $\text{cm}^{-1}$  can be observed and this is the characteristics vibration band of acrylic resin contributed by CH<sub>3</sub> and O-CH<sub>2</sub> bending. The molecular structure of acrylic resin coating with the corresponding vibration mode is tabulated in Table 3.

TABLE 3. Colour coded IR absorption assigned to its corresponding vibration

Wavenumber ( $\text{cm}^{-1}$ )	Corresponding vibration	Molecule
1166, 1195, 1261	C-C-O-C stretching	
1454	CH <sub>2</sub> , $\alpha$ -CH <sub>3</sub> and (O)CH <sub>3</sub> bending	
1494	$\alpha$ -CH <sub>3</sub> asymmetric deformation	
1729	C=O stretching	



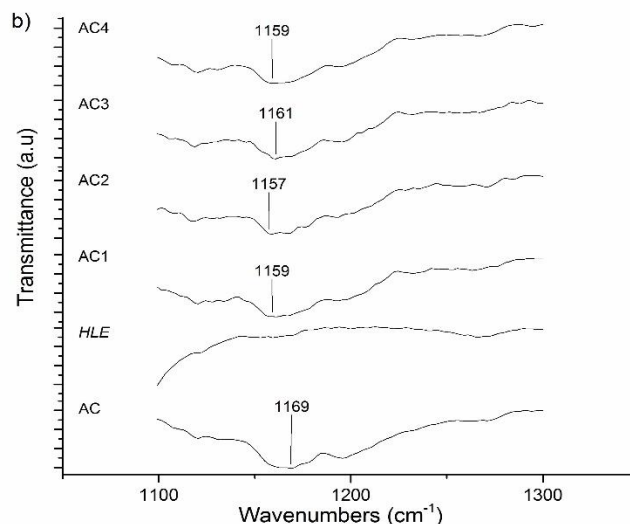


FIGURE 1. IR spectra of the coating system at a) overall spectra b)  $1100\text{ cm}^{-1} - 1300\text{ cm}^{-1}$

The incorporation of HLE in AC has reduced the intensity of C-H stretching vibration as seen in region 1 ( $2805 - 3150\text{ cm}^{-1}$ ). This indicates that the concentration of the corresponding functional group was reduced due to the dissociation of the polymer chain. In region 2 ( $1320 - 1815\text{ cm}^{-1}$ ), the following corresponding vibration namely as  $\text{CH}_2$ ,  $\alpha\text{-CH}_3$  and  $(\text{O})\text{CH}_3$  bending ( $1378, 1454\text{ cm}^{-1}$ ),  $\alpha\text{-CH}_3$  asymmetric deformation ( $1494\text{ cm}^{-1}$ ) as well as C=O stretching ( $1729\text{ cm}^{-1}$ ) can be observed. Note that these peaks show a reduction in intensity indicating that the acrylic resin polymer backbone has been dissociated while HLE has been associated in the polymer to form a complexation.

Figure 1b shows an IR frequency at  $1168\text{ cm}^{-1}$  for acrylic coating and it was observed to reduce to  $1157 - 1160\text{ cm}^{-1}$ . This peak which attributed to the acrylic coating C-C-O-C stretching vibration reduced after incorporation of HLE indicates the chain scission of the methoxycarbonyl group ( $\text{COOCH}_3$ ) from acrylic coating. Chain scission of the acrylic coating provides a reaction of this group with another molecule and resulting in the change of polymer properties.

The deconvoluted FTIR spectra of AC2 coating in the range of  $1560 - 1720\text{ cm}^{-1}$  is shown in Figure 2. This area becomes one of the interest regions due to the availability of the carbonyl C=O functional group. It can be seen that in the region of  $1560 - 1700\text{ cm}^{-1}$ , there are 3 main peaks which contribute to the presence of carbonyl group (C=O) and C=C bond. The carbonyl group of HLE and AC was found at  $1633\text{ cm}^{-1}$  and  $1729\text{ cm}^{-1}$ , respectively. Incorporation of HLE has shifted carbonyl (C=O) peaks to a higher wavelength of  $1636\text{ cm}^{-1}$  and  $1665\text{ cm}^{-1}$ , respectively. This is due to the association of the carbonyl group of lawsone with the acrylic resin polymer. This association is assisted by hydrogen

bonding where it primarily depends on the presence of C-O and C=O functional group. The hydrogen bonding of HLE and AC is modelled in Figure 3.

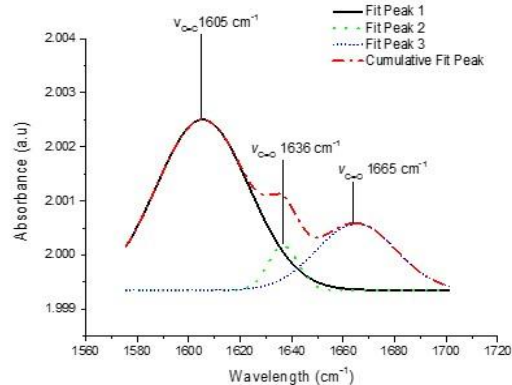


FIGURE 2. FTIR deconvolution of AC2 at C=O region

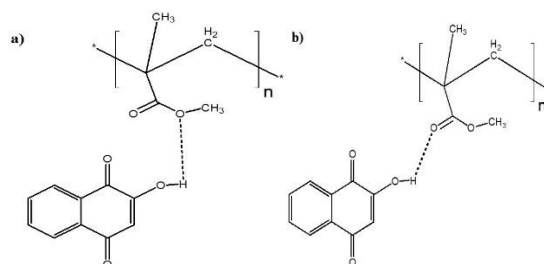


FIGURE 3. A proposed hydrogen bonding between acrylic and HLE a) at C-O b) at C=O

#### Water Permeability Study

Water permeability of acrylic resin with incorporation of HLE is shown in Figure 4. The

water permeability was found to decrease greater than acrylic resin itself. The decrease of water flux is associated with the hydrophobicity of the coating. AC2 coating shows the lowest water permeability while AC coating shows the highest water permeability. All coating samples show a reduction in water permeability. The structural changes are described by the packing particle of the colloidal system since penetration of water is through the defect like pores and cracks (Reyes-Mercado et al., 2008). Due to the reduction of the attracting force in the coating molecules which consequently reduces the surface tension, the structure of the acrylic resin coating has changed. The addition of HLE has caused a reduction in water permeability due to the compact structure and high density of the colloidal system. Acrylic coating shows a hydrophobic behaviour due to its ethyl functional group. The structural changes due to the addition of HLE have caused an increment in hydrophobicity of the acrylic resin.

AC3 and AC4 only represent one time constant while AC1 shows an increasing spike in the low frequency region. The formation of second time constant is more obvious in sample AC2 as seen in Figure 5b. In the lower frequency, the plot of  $-Z''$  versus  $Z'$  deviates from  $Z'$  axis indicating that the diffusion process needs to be considered in simulating the equivalent circuit. The equivalent circuit was constructed based on this basis and shown in Figure 5.

An electrochemical circle fit was used to determine the value of coating resistance ( $R_c$ ) and the corresponding values are tabulated in Table 4.  $R_c$  value for all tested samples is above the magnitude of  $10^7$  and this magnitude is a threshold value for a good coating (Sathiyarayanan et al. 2007).  $R_c$  was found to increase from AC to AC2 and further addition of HLE after that has caused the reduction in  $R_c$  value. The crystalline structure of AC2 limits the ionic mobility through the pores and reduces the electrical conductivity on the aluminium surface.

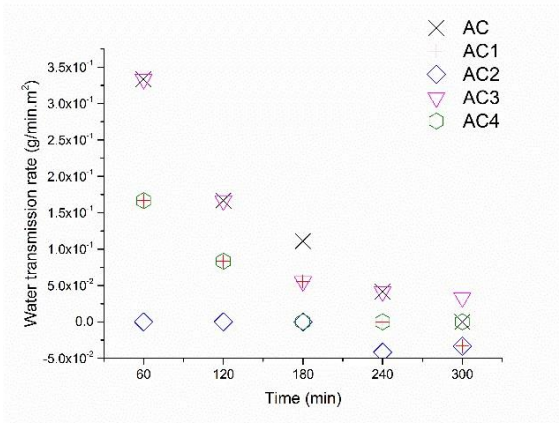


FIGURE 4. Water Vapor permeability of AC in the presence and absence of HLE

*Electrochemical impedance spectroscopy (EIS)*

Nyquist plot is depicted in Figure 5a and b to show the impedance spectra of acrylic resin coating in the absence and presence of HLE. As seen, samples AC,

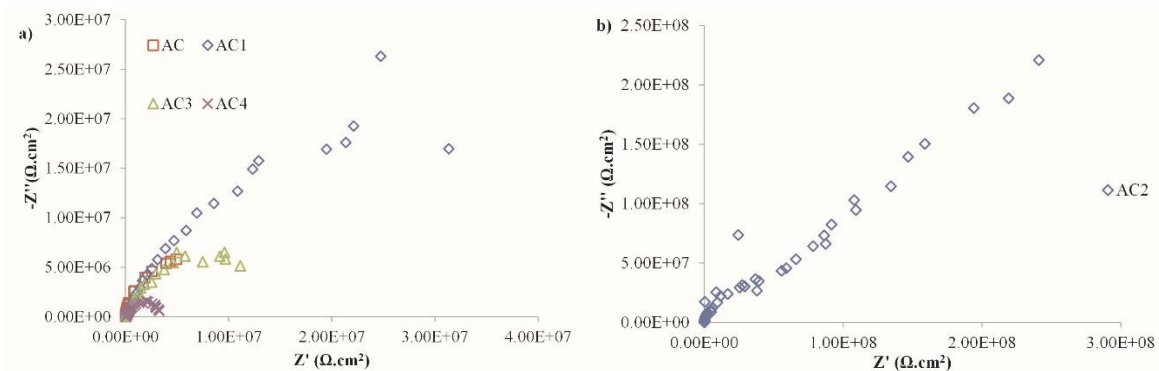


FIGURE 5. Nyquist plot for a) AC, AC1, AC3 and AC4 b) AC2

TABLE 4. Corresponding values gained from impedance analysis

Parameters	Coating				
	AC	AC1	AC2	AC3	AC4
$R_c$ ( $\Omega \cdot \text{cm}^2$ )	9.28E+06	4.53E+07	4.79E+08	2.06E+07	4.08E+06
$C_c$ (F/cm <sup>2</sup> )	2.00E-08	1.15E-08	3.32E-09	7.73E-08	8.18E-08
$ Z _{\text{lf}}$ ( $\Omega$ )	4.40E+07	3.13E+07	2.30E+08	1.15E+07	3.38E+06

Theoretically, the coating capacitance is represented by  $C_c = \varepsilon \varepsilon_0 A/d$  where  $\varepsilon$  is a dielectric constant of the medium,  $\varepsilon_0$  is the free space permittivity,  $A$  is the testing area and  $d$  is the coating thickness (Dong & Zhou, 2014).  $C_c$  is an important parameter because of the water barrier property is a crucial element in which the presence of aqueous solution will start the corrosion process (Mansfeld, 1990). The value of  $C_c$  was found to decrease when the HLE was loaded into the acrylic coating. For AC2 sample, the  $C_c$  was decreased to one order of magnitude. In general, greater  $C_c$  value leads to the increment of water uptake to the coating film and the ideal value of  $C_c$  that shows an excellent coating behaviour is usually less than 1nF. The amorphous structure provides a greater ionic diffusivity which latter causing increasing in ionic conductivity. The decreasing of  $C_c$  is an indicator of low absorption of the water into the coated substrate (Yasakau et al. 2008). Coating capacitance represents water barrier property of the organic coating. Modulus of impedance at low frequency  $|Z|_{\text{lf}}$  is shown in Table 4. The value is recorded at 0.1Hz where this is the lowest frequency used in the EIS measurement. The similar trend with  $R_c$  can be seen in which the value increases from AC to AC2 and after that showing a reduction trend beyond AC2. The value of  $|Z|_{\text{lf}}$  is almost similar to the value of  $R_c$  because of it has reached the dc limit where  $|Z| \approx R_c$  because  $|Z| = \sqrt{Z_{\text{real}}^2 + Z_{\text{img}}^2}$  and  $\lim_{f \rightarrow 0} (Z_{\text{real}})_{E=E_{oc}} = R_p + R_\Omega$  and  $\lim_{f \rightarrow 0} (Z_{\text{img}}) = 0$  (Mansfeld, 2005).

A circuit was constructed regarding to the semi-infinite diffusion case where the diffusion element is represented by Warburg element,  $W$  as shown in Figure 6. The constructed circuit consist of three time constants namely as  $(R_f Q_{dl})$ ,  $(R_{ct} Q_{dl})$  and  $(W)$  Finšgar & Jackson, 2014; Grundmeier et al. 2000; Mansfeld, 2005; Bisquert et al. 1999; Ashassi-Sorkhabi et al. 2008). These time constants are connected in series with uncompensated resistance,  $R_\Omega$  which occurred due to solution resistance.

At high frequency region  $(R_f Q_{dl})$ , the dissolution of aluminium ions trough the surface layer occurred.  $R_f$  represents the resistance of the ion conduction path which was developed in the surface layer.  $R_f$  value for AC is the highest due to its high surface layer resistance contributed by low pores and conduction pathways. AC1 – AC4 have low  $R_f$  value due to the distribution of small number of HLE on the coating surface. The first time constant can be attributed to the process occurred at the metal - electrolyte interface covered by an acrylic resin coating. At this stage, a pocket filled with electrolyte can be found where the electrolyte contained in this pocket is different from the bulk electrolyte outside the coating layer.  $Q_{dl}$  value for AC2 is the lowest ( $5.03 \times 10^{-10}$  F/cm<sup>2</sup>) indicating low electrolyte collection at the coating-pocket solution interface. The second time constant is represented by  $(R_{ct} Q_{dl})$  and located in the low frequency region. As seen in Table 5, the value of  $R_{ct}$  increases from AC to AC2, followed by a reduction afterwards.  $R_{ct}$  of AC2 shows highest value ( $4.66 \times 10^7 \Omega$ ) indicating that it has limited the charge transferred when an electron enters the metal and metal ions diffused into the electrolyte.  $Q$  is the constant phase element (CPE) and represents the double layer capacitor which usually related to the water barrier property of the coating. AC1-AC4 shows lower  $Q$  value in comparison to AC due to low water uptake at the metal-coating interface. Incorporation of HLE has limited the water uptake due to its close pack structure formation between HLE and acrylic resin. The third time constant is  $W$  that represents the elements of semi-infinite layer thickness diffusion. The diffusion speed is characterized by the impedance of the diffusion process. The higher value of  $W$  attributes to the higher speed of diffusion. The lowest value of  $W$  is recorded by AC2 ( $1.21 \times 10^{-7} \Omega \cdot \text{s}^{1/2}$ ) which signifies better impedance at this stage. The existence of Warburg impedance is also an indication of the considerable barrier formation from corrosion attack (Weng et al. 1997).

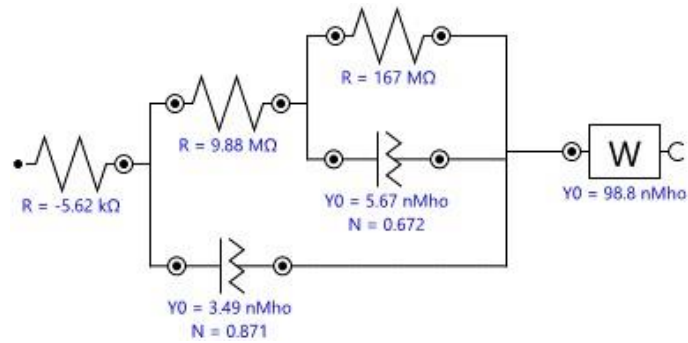


FIGURE 6. An equivalent circuit constructed for all coating systems

TABLE 5. Impedance parameters for AA5083 in seawater at various loadings of HLE

Parameter	Coating system				
	AC	AC1	AC2	AC3	AC4
$R_{\Omega}$	23982	10095	-7844.4	5987.8	7097.5
$R_f$	$5.25 \times 10^7$	$6.32 \times 10^4$	$4.47 \times 10^5$	$3.96 \times 10^5$	$1.31 \times 10^4$
$Q_{dl}/C$	$1.71 \times 10^{-9}$	$7.33 \times 10^{-10}$	$5.03 \times 10^{-10}$	$2.40 \times 10^{-8}$	$4.62 \times 10^{-9}$
$Q/C_{dl}$	$3.59 \times 10^{-10}$	$2.26 \times 10^{-8}$	$9.20 \times 10^{-9}$	$4.04 \times 10^{-8}$	$1.17 \times 10^{-7}$
n	-	0.79454	0.61876	0.52548	1.0727
$R_{ct}$	$1.68 \times 10^6$	$4.49 \times 10^7$	$4.66 \times 10^8$	$1.47 \times 10^7$	$1.43 \times 10^6$
W	$1.64 \times 10^{-7}$	$2.71 \times 10^{-7}$	$1.21 \times 10^{-7}$	$4.12 \times 10^{-7}$	$5.10 \times 10^{-7}$
$\chi^2$	5.9517	0.14729	0.012841	0.24202	0.52533

The mechanism of acrylic resin coating in AC2 and AC4 is shown in Figure 7. In AC2 system, the molecular arrangement is in order structured due to its semi-crystalline nature as reported in our previous research elsewhere (Zulkifli et al. 2017). The ordered structure of HLE in acrylic resin coating was built in a close pack structured which providing a greater barrier effect. Whilst in AC4 system, the excessive HLE has caused a formation of less semi-crystalline structured. This might be due to the excessive HLE that are not cross linked with the acrylic polymer chain. Consequently, the mixture of acrylic resin coating and HLE has formed an amorphous mixture where the HLE molecules coordination is in a random order. Hence the seawater is easy to penetrate the coating compared to AC2 which has a close pack molecular order to block the penetration of seawater.

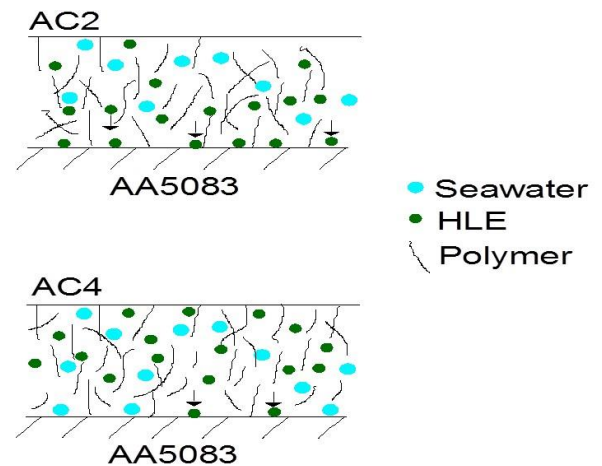


FIGURE 7. Suggested mechanism of acrylic resin coating incorporated with HLE

#### CONCLUSION

The incorporation of HLE in acrylic coating and its subsequent effect was investigated at ambient temperature. Optical, electrochemical and mechanism studies were conducted to assess the effect of concentration variations of HLE in acrylic

resin coating. Upon addition of HLE, chain scission between HLE and acrylic resin has occurred and caused a formation of hydrogen bonding between both substances. AC2 excellently impeded the corrosion attack by forming a close pack structure and the mechanism of the modified acrylic resin coating was suggested. This close pack structure has caused the formation of semi-crystalline structure which provides greater barrier effect and hence reduces corrosion attack. The highest coating resistance was found at AC2 and it is inferred that this is the best concentration to be used in the coating system.

#### ACKNOWLEDGEMENT

The authors would like to express their gratitude for the funds and scholarship provided by Ministry of Education, Malaysia (Look East Policy Grant Vot 53168; FRGS Vot 59210 & MyPhD) and Miss Suria Hani from English Learning Centre for her proofreading service.

#### REFERENCES

- Abulyazid I., Mahdy, E.M.E., & Ahmed, R.M. 2013. Biochemical study for the effect of henna (*Lawsonia inermis*) on *Escherichia coli*. *Arabian Journal of Chemistry* 6: 265–273.
- Akbarinezhad, E., Ebrahimi, M., Sharif, F., & Ghanbarzadeh, A. 2014. Evaluating protection performance of zinc rich epoxy paints modified with polyaniline and polyaniline-clay nanocomposite. *Progress in Organic Coatings* 77: 1299–1308.
- Ashassi-Sorkhabi, H., Seifzadeh, D., & Hosseini, M.G. 2008. EN, EIS and polarization studies to evaluate the inhibition effect of 3H-phenothiazin-3-one, 7-dimethylamin on mild steel corrosion in 1M HCl solution. *Corrosion Science* 50: 3363–3370.
- Ashjari, M., Mostafapour Asl, A., & Rouhi, S. 2015. Experimental investigation on the effect of process environment on the mechanical properties of AA5083/Al2O3 nanocomposite fabricated via friction stir processing. *Materials Science and Engineering: A* 645: 40–46.
- Bisquert, J., Garcia-Belmonte, G., Fabregat-Santiago, F., & Bueno, P.R. 1999. Theoretical models for ac impedance of finite diffusion layers exhibiting low frequency dispersion. *Journal of Electroanalytical Chemistry* 475: 152–163.
- Buchweishaija, J. 2009. Phytochemicals As Green Corrosion Inhibitors in Various Corrosive Media: a Review. *Tanzania Journal of Science* 35: 77–92.
- Dong, Y., & Zhou, Q. 2014. Relationship between ion transport and the failure behavior of epoxy resin coatings. *Corrosion Science* 78: 22–28.
- Finšgar, M., & Jackson, J. 2014. Application of corrosion inhibitors for steels in acidic media for the oil and gas industry: A review. *Corrosion Science* 86: 17–41.
- Gaaz, T. S., Hussein, E. K., & Al-Amiery, A. A. 2017. Physical Properties of Halloysite Nanotubes-Polyvinyl Alcohol Nanocomposites Using Malonic Acid Crosslinked. *Jurnal Kejuruteraan* 29(2): 71–77.
- Grundmeier, G., Schmidt, W., & Stratmann, M. 2000. Corrosion protection by organic coatings: electrochemical mechanism and novel methods of investigation. *Electrochimica Acta* 45: 2515–2533.
- Jeyaseelan, E.C., Jenothiny, S., Pathmanathan, M., & Jeyadevan, J. 2012. Antibacterial activity of sequentially extracted organic solvent extracts of fruits, flowers and leaves of *Lawsonia inermis* L. from Jaffna. *Asian Pacific Journal of Tropical Biomedicine* 2: 798–802.
- Khaled, K.F., & Hackerman, N. 2003. Investigation of the inhibitive effect of ortho-substituted anilines on corrosion of iron in 1 M HCl solutions. *Electrochimica Acta* 48: 2715–2723.
- Kucera, S., Shah, N.H. Malick, A.W., Infeld, M.H., & McGinity, J.W. 2009. Influence of an acrylic polymer blend on the physical stability of film-coated theophylline pellets. *AAPS PharmSciTech* 10: 864–871.
- Mansfeld, F. 1990. Electrochemical impedance spectroscopy (EIS) as a new tool for investigating methods of corrosion protection. *Electrochimica Acta* 35: 1533–1544.
- Mansfeld, F. 2005. Tafel slopes and corrosion rates obtained in the pre-Tafel region of polarization curves. *Corrosion Science* 47: 3178–3186.
- Motalebi, A., Nasr-Esfahani, M., Ali, R., & Pourriahi, M. 2012. Improvement of corrosion performance of 316L stainless steel via PVTMS/henna thin film. *Progress in Natural Science: Materials International* 22: 392–400.
- Ostovari, A., Hoseinie, S.M., Peikari, M., Shadizadeh, S.R., & Hashemi, S.J. 2009. Corrosion inhibition of mild steel in 1M HCl solution by henna extract: A comparative study of the inhibition by henna and its constituents (Lawsone, Gallic acid,  $\alpha$ -D-Glucose and Tannic acid). *Corrosion Science* 51: 1935–1949.
- Othman, K., Ghani, J. A., Haron, C. H. C., Juri, A., & Kassim, M. S. 2018. Microstructural Study of Aluminium Alloy A390 after Milling



- Process. *Jurnal Kejuruteraan* 30(2): 257-264.
- Papaj, E.A., Mills, D.J., & Jamali, S.S. 2014. Effect of hardener variation on protective properties of polyurethane coating. *Progress in Organic Coatings* 77: 2086–2090.
- Rajendran, S., Agasta, M., Bama Devi, R., Shyamala Devi, B., Rajam, K., & Jayasundari, J. 2009. Corrosion inhibition by an aqueous extract of Henna leaves (*Lawsonia Inermis* L). *Zaštita Materijala* 50: 77–84.
- Reyes-Mercado, Y., Vázquez, F., Rodríguez-Gómez, F.J., & Duda, Y. 2008. Effect of the acrylic acid content on the permeability and water uptake of poly (styrene-co-butyl acrylate) latex films. *Colloid and Polymer Science* 286: 603–609.
- Salunke-Gawali, S., Kathawate, L., Shinde, Y., Puranik, V.G., & Weyhermüller, T. 2012. Single crystal X-ray structure of Lawsone anion: Evidence for coordination of alkali metal ions and formation of naphthosemiquinone radical in basic media. *Journal of Molecular Structure* 1010: 38–45.
- Samsudin, A.S., Khairul, W.M., & Isa, M.I.N. 2012. Characterization on the potential of carboxy methylcellulose for application as proton conducting biopolymer electrolytes. *Journal of Non-Crystalline Solids* 358: 1104–1112.
- Sathiyarayanan, S., Azim, S.S., & Venkatachari, G. 2007. A new corrosion protection coating with polyaniline–TiO<sub>2</sub> composite for steel. *Electrochimica Acta* 52: 2068–2074.
- Weng, D., Jokić, P., Uebles, A., & Boehni, H. 1997. Corrosion and protection characteristics of zinc and manganese phosphate coatings. *Surface and Coatings Technology* 88: 147–156.
- Yasakau, K.A., Zheludkevich, M.L., Karavai, O. V., & Ferreira, M.G.S. 2008. Influence of inhibitor addition on the corrosion protection performance of sol–gel coatings on AA2024. *Progress in Organic Coatings* 63: 352–361.
- Zulkifli, F., Yus of, M.S.M., Isa, M.I.N., Yabuki, A., & Nik, W.B. 2017. Henna leaves extract as a corrosion inhibitor in acrylic resin coating. *Progress in Organic Coatings* 105: 310-319.

